Nanoscale

Dynamic Article Links

Cite this: *Nanoscale*, 2011, **3**, 3064

www.rsc.org/nanoscale

COMMUNICATION

$(AuAg)_{144}(SR)_{60}$ alloy nanomolecules

Chanaka Kumara and Amala Dass*

Received 28th April 2011, Accepted 23rd May 2011
DOI: 10.1039/c1nr10429b

$(Au\text{-}Ag)_{144}(SR)_{60}$ alloy nanomolecules were synthesized and characterized by ESI mass spectrometry to atomic precision. The number of Ag atoms can be varied by changing the incoming metal ratio and plateaus at ~60. UV-vis data demonstrates that the electronic structure of the nanomolecules can be tuned by incorporation of silver atoms. Based on the proposed 3-shell structure of $Au_{144}(SR)_{60}$, we hypothesize that the Ag atoms are selectively incorporated in to the symmetry equivalent 60-atom shell—having Au_{12}, Au_{42}, Ag_{60} concentric shells with 30 –SR–Au–SR– protecting units.

Ultra-small gold nanoparticles that are <2 nm are molecular in nature—they have unique molecular weights, physical and chemical properties.[1] Typical examples of nanomolecules with specific number of gold atoms and organic thiol ligands include $Au_{25}(SR)_{18}$, $Au_{38}(SR)_{24}$, $Au_{102}(SR)_{44}$ and $Au_{144}(SR)_{60}$.[2–5] Metallic Au nanomolecules are attractive due to their chemical stability and the ability to characterize these materials precisely using commercially available mass spectrometers, NMR and a variety of spectroscopic instruments.[6,7] $Au_{25}(SR)_{18}$ and $Au_{144}(SR)_{60}$ have been studied extensively due to their exceptional stability and optical properties.[8–11] Ag nanoparticles have interesting optical properties[12,13] and promising anti-bacterial and anti-fungal activity.

While monometallic nanomolecules are extremely stable, and are easily processed and characterized, alloys have unique advantages such as enhanced catalytic activity.[14] In terms of Au-metal containing alloy nanoparticles, Murray *et al.*[15] synthesized a 3–5 nm monolayer protected metal alloy by doping Au with Ag, Cu and Pt. El-Sayed *et al.*[16] showed the formation of ~20 nm gold–silver alloy nanoparticles with different compositions by co-reduction of Au and Ag precursors in varying proportions with sodium citrate. Murphy *et al.*[17] reported the synthesis of sub-10 nm alloy nanoparticles. Wilcoxon[18] studied the optical properties of Au–Ag alloy nanoparticles and their dependence on composition and size. These reports, mostly in the 3–20 nm size regime show that the Au–Ag nanomaterials are indeed alloys and that the position of the SPR band depends on the ratio of Au and Ag starting precursors.[12,13,16–19]

Ultra-small nanoclusters (<2 nm) have been doped with Pd and Ag. For example, monolayer protected Au–Pd clusters have been initially synthesized by Murray *et al.*[20] and $Au_{24}Pd(SCH_2CH_2Ph)_{18}$ clusters isolated by Negishi *et al.*[21] Optical and electrical properties of Au_{25} can be tuned by doping Pd into the Au core. Recently Negishi *et al.*[22] reported the synthesis of $Au_{25-x}Ag_x$ $(SR)_{18}$ in the range of 6–8 kDa cluster size, showing that the electronic structure can be modulated by the incorporation of Ag atoms into Au_{25} core.

Here, we report the synthesis and isolation of $(Au–Ag)_{144}(SR)_{60}$ alloy nanomolecules and characterize them by ESI mass spectrometry to the atomic level. From the molecular weight information obtained by ESI, and hence the exact number of Au and Ag atoms, we show that the Ag incorporation into the nanoalloy does not depend linearly with the Ag ratio of the starting material. UV-visible spectroscopy shows the Ag incorporation affects the electronic structure of the nanomolecules. We discuss the Ag incorporation into the Au_{144} nanomolecules based on a proposed crystal structure.[10]

Materials and method

Synthesis

Synthesis of the $(Au\text{-}Ag)_{144}(SR)_{60}$ involves two steps. The first step is the synthesis of crude product that contains polydisperse Au–Ag clusters according to Negishi *et al.*[22] The second step is the etching of the crude product with excess thiol to form $(Au–Ag)_{144}$ alloy nanomolecules.

Step 1: Aqueous solution (30 mL) containing $HAuCl_4$ and $AgNO_3$ (total metal concentration was set to 30 mM) was mixed with toluene solution (30 mL) of tetraoctylammonium bromide, TOABr (1.1 mmol). The initial mole ratios of Au : Ag precursors were 1 : 0, 1 : 0.25, 1 : 0.5, 1 : 0.66 or 1 : 0.75. After stirring for 30 min, the turbid organic phase was separated and phenylethane thiol (10 mmol) was added and further stirred for 30 min at room temperature. This solution was cooled in ice bath for 30 min. An aqueous solution of $NaBH_4$ (20 mmol, 20 mL) cooled to 0 °C, was rapidly added to the reaction mixture under vigorous stirring. After 3 h, the organic layer was separated from aqueous layer and evaporated to dryness. The product was washed with methanol to remove excess thiol, $NaBH_4$, TOABr and other by-products. The residual mixture was extracted with toluene. Smaller clusters in the 7–10 kDa range were removed by CH_3CN extraction.

Step 2: 20 mg of CH_3CN insoluble portion was dissolved in 0.5 ml of toluene and etched with excess phenylethane thiol (0.5 mL) at 80 °C under stirring, while monitoring with MALDI MS. When pure $(Au–Ag)_{144}$ nanoalloy was formed (~3h), the reaction was stopped and washed with methanol. The toluene soluble fraction of the product was subjected to further analysis. Full synthetic details are

Department of Chemistry and Biochemistry, University of Mississippi, 352 Coulter Hall, University, 38677 Mississippi, USA. E-mail: amal@olemiss.edu; Fax: +1 662 915 7300; Tel: +1 915 7301

beyond the scope of this work and will be reported in a separate synthetic report.

Spectroscopy/mass spectrometry

UV-Visible spectra were obtained in dichloromethane solutions using Shimadzu UV-1601 spectrophotometer/UV probe 2.0 software in the 300–1200 nm range. MALDI mass spectra were acquired with a Bruker Daltonics Autoflex mass spectrometer using DCTB matrix[23] at optimal laser fluence. Positive and negative mode gave identical results. Spectral analyses were done using Bruker Daltonics flexAnalysis version 3.0. ESI mass spectra were obtained from a Waters Synapt mass spectrometer in 50 : 50 toluene : CH_3CN solution in negative mode. ESI calibration was performed with 50 : 50 isopropanol : water solution of NaI. Calibration check was performed with $Au_{25}(SCH_2CH_2Ph)_{18}$ and $Au_{144}(SCH_2CH_2Ph)_{60}$.

Results and discussion

Electrospray ionization mass spectra of the Au–Ag nanomolecules show that the composition of the nanoalloys is $(Au–Ag)_{144}(SR)_{60}$ where the Au–Ag ratio varies with the incoming mol ratio of $HAuCl_4$ and $AgNO_3$.

Fig. 1 shows the mass region focused on the 3- ions of the nanomolecules that were predominant in the ESI experiments. The bottom black curve shows the monometallic $Au_{144}(SR)_{60}$ that has extraordinary stability among various monometallic nanomolecules. Incorporating silver precursor, $AgNO_3$ in the synthesis led to the formation of $Au_xAg_y(SR)_{60}$ nanoalloys while the core size was maintained at 144 total atoms, *i.e.*, $x + y = 144$. The distribution of peaks is due to the different number of Au and Ag atoms as denoted by the 89 Da mass difference between the peaks (Au = 196.97 Da, Ag = 107.87 Da, Δm = 89.1 Da). The fraction of Ag atoms in the nanoalloy product does not reflect the mole fraction of the precursor starting materials, $HAuCl_4$ and $AgNO_3$ as discussed later. The silver fraction in the nanoalloy seems to plateau at 37% for the 1 : 0.75 Au : Ag incoming mole ratio. Experiments at higher silver ratios (*e.g.*, 1 : 1 Au : Ag) do not lead to stable $(Au–Ag)_{144}$ alloy formation. Synthesis from 1 : 0.25 Au : Ag mole ratio also form $(Au–Ag)_{145}(SR)_{59}$ alloys as a minor fraction. The distribution of peaks in each incoming ratio synthesis remains constant at ~11 and ~7 at baseline and FWHM of each envelope, reminiscent of binomial distribution found in ligand exchange experiments reported earlier.[24]

Are these $(Au–Ag)_{144}$ nanomolecules monodisperse?

MALDI TOF mass spectrometry, a hard ionization source, especially at high laser fluence, easily ionizes a variety of analytes. This makes MALDI data more suitable for mixtures and hence facilitates attaining a more accurate representation of the nanomaterial composition.[25–27] Ionization in electrospray spray can be selective depending on the spray conditions. Fig. 2 shows the MALDI MS data of the $(Au–Ag)_{144}$ nanomolecules and confirms their purity and

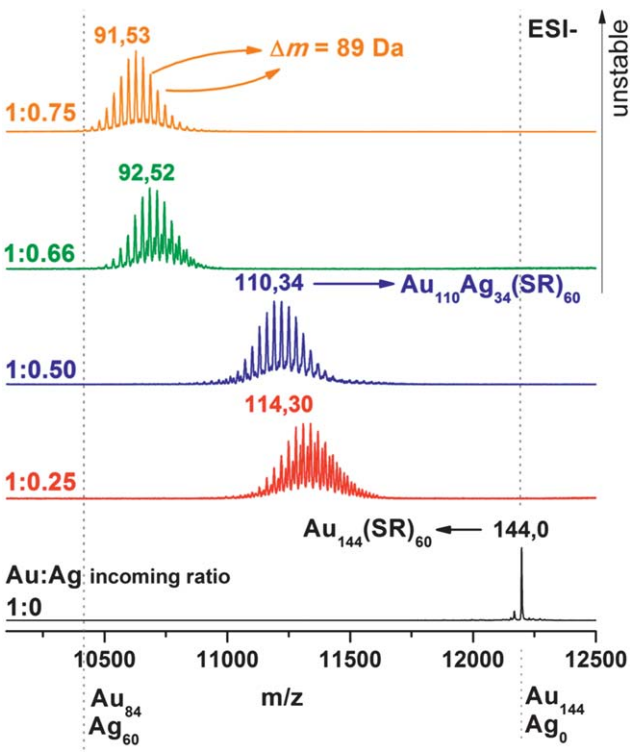

Fig. 1 Electrospray ionization (ESI) mass spectrometry data (3- ions) of $(Au–Ag)_{144}(SR)_{60}$ nanomolecules for Au : Ag precursor ratios of 1 : 0 (black), 1 : 0.25 (red), 1 : 0.50 (blue), 1 : 0.66 (olive) and 1 : 0.75 (orange) in the starting material. Samples were infused as 50 : 50 toluene : CH_3CN solution in negative mode. The mass difference between the peaks in nanoalloys corresponds to the Au (196.97 Da) and Ag (107.87 Da) mass difference, Δm = 89 Da. Average number of Au and Ag atoms is denoted above each distribution of peaks.

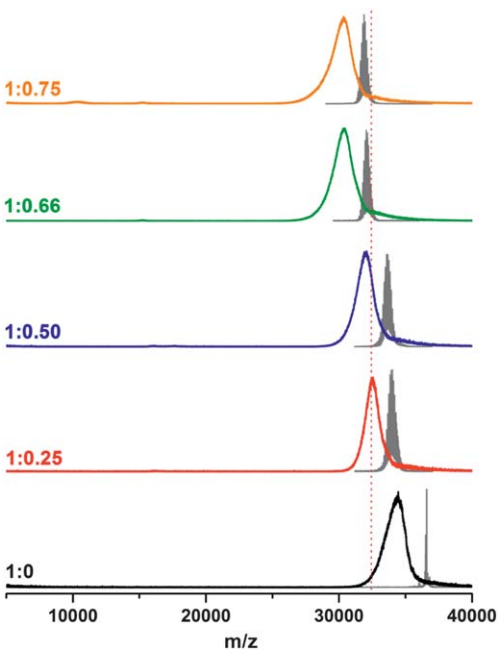

Fig. 2 MALDI TOF mass spectra (positive mode) of $(Au–Ag)_{144}(SR)_{60}$ nanomolecules for Au : Ag precursor ratios of 1 : 0 (black), 1 : 0.25 (red), 1 : 0.50 (blue), 1 : 0.66 (olive) and 1 : 0.75 (orange) in the starting material. The 3- ESI mass spectra from Fig. 1 was deconvoluted and plotted as 1- peaks in grey. The MALDI peaks are significantly broader and slightly lower in mass than ESI peaks due to fragmentation from the loss of ligands. Toluene solution of the (Au–Ag) nanoclusters were mixed with DCTB matrix in toluene and air dried in steel plate for MS analysis.

monodispersity. The 3- ESI peaks from Fig. 1 are deconvoluted to 1- ions (grey peaks) and plotted along with MALDI 1+ ions as shown in Fig. 2. The MALDI peaks are significantly broader and slightly lower in mass due to fragmentation from the loss of ligands by the breakage of S–C bonds.[28]

Tuning the electronic structure of the nanoalloys

Optical properties of nanoalloys including Au–Ag have been intensely studied especially the effect of the proportion of Ag metal on the surface plasmon resonance (SPR) peak, where the core sizes of nanoalloys are in the 5–50 nm diameter range.[12–14,16–19] Nanoparticles that are less than 2 nm in diameter, however, show distinct features instead of SPR peaks, due to quantum size effects.[29,30] These features are size dependent and are less distinct with larger sizes such as Au_{144} before the emergence of an SPR peak for nanoclusters around 5 nm in diameter. While the optical spectrum of monometallic Au_{144} nanomolecules is relatively monotonous, Ag incorporation to form $(Au–Ag)_{144}$ nanoalloys affects the electronic structure and leads to a ~425 nm peak reminiscent of the silver SPR band[13] and broad shoulders at 560 and 310 nm (Fig. 3).

We also show that these $(Au–Ag)_{144}$ alloy nanomolecules can be synthesized with various protecting thiol groups such as phenylethane thiol, dodecane thiol and hexane thiol, though the pK_a of these thiols should be very similar. Fig. 4 demonstrates the reproducibility of the $(AuAg)_{144}(SR)_{60}$ nanoalloy formation during the synthesis.

The structure arrangement of atoms in $Au_{144}(SR)_{60}$ most likely is similar to the experimental XRD crystal structure of $Pd_{145}(CO)_x(PEt_3)_{30}$[10,31–33] The proposed $Au_{144}(SR)_{60}$ structure shows a good fit with the experimental X-ray scattering data. The relaxed structure shows three concentric shells of 12, 42 and 60 atoms protected by 30 –SR–Au–SR– staple groups. As the silver mole ratio is increased in the starting material, the number of Ag atoms in the $(Au–Ag)_{144}$ alloy increases as expected. However the Ag atoms seem to plateau around 1 : 0.66 Au : Ag incoming mole ratio. The average and maximum number of Ag atoms in both the 1 : 0.66 and 1 : 0.75 ratios are ~52 and ~60 respectively. Based on the crystal structure prediction, there are two possible options for Ag atom incorporation: 1) The Ag atoms are present both in the staple units as –SR–Ag–SR– and partially occupy the equivalent 60 atom shell; 2) The staple units have Au atoms, but Ag atoms are only exclusively incorporated into the equivalent 60 atom shell. Case 1 cannot account for the pleateau of 60 Ag atoms, while case 2 does. However, the selective incorporation of Ag atoms in the outmost shell and not the protecting staple units could not be explained. Synthesis using a high Ag precursor ratio such as 1 : 1 Au : Ag mole ratio leads to unstable clusters in the 144 atom region. This suggests that a high number of Ag atoms are incorporated during the synthesis, but it is not stable. Modeling of these alloys will provide insights in to the stability and selection of alloy metal ratio. Regardless, the reported $(Au–Ag)_{144}$ alloys has greater potential for interesting catalytic applications compared to analogous monometallic nanomolecules.

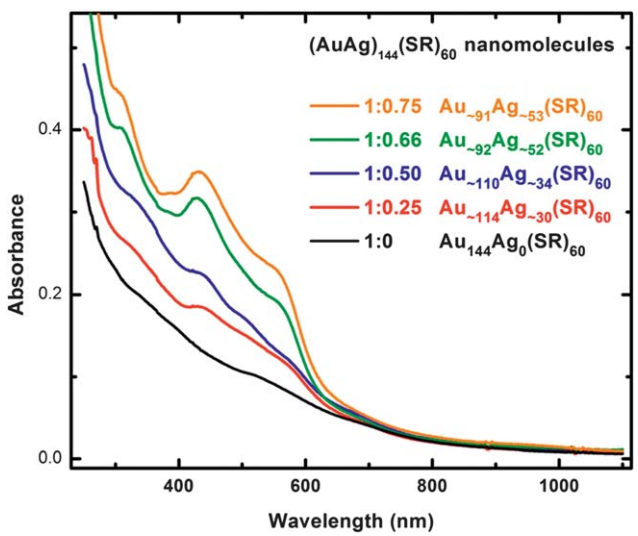

Fig. 3 UV-vis spectra of $(Au–Ag)_{144}(SR)_{60}$ nanomolecules in CH_2Cl_2 for Au : Ag precursor ratios of 1 : 0 (black), 1 : 0.25 (red), 1 : 0.50 (blue), 1 : 0.66 (olive) and 1 : 0.75(orange) in the starting material.

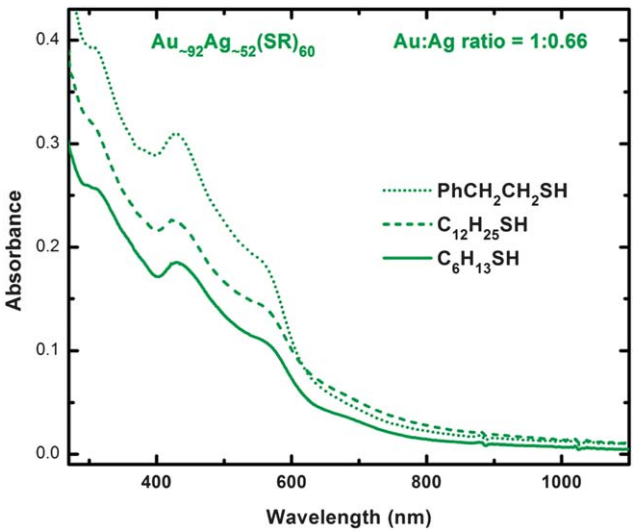

Fig. 4 UV-vis spectra of $Au_{\sim92}Ag_{\sim52}(SR)_{60}$ nanomolecules for Au : Ag precursor ratios of 1 : 0.66 with phenylethane thiol (dotted), hexane thiol (dashed), and dodedane thiol (solid).

Acknowledgements

We gratefully acknowledge support from NSF 0903787, and the University of Mississippi Startup Fund. We thank Charles Hussey, Glenn Hopkins, Jordan Blodgett and the Office of Research and Sponsored Programs for Bruker Autoflex MALDI TOF and Waters Q-TOF SYNAPT instrumentation; Hannu Hakkinen, and James Cizdziel for sharing optimized structures and helpful discussions.

References

1 R. L. Whetten, J. T. Khoury, M. M. Alvarez, S. Murthy, I. Vezmar, Z. L. Wang, P. W. Stephens, C. L. Cleveland, W. D. Luedtke and U. Landman, *Adv. Mater.*, 1996, **8**, 428–433.
2 P. D. Jadzinsky, G. Calero, C. J. Ackerson, D. A. Bushnell and R. D. Kornberg, *Science*, 2007, **318**, 430–433.
3 M. W. Heaven, A. Dass, P. S. White, K. M. Holt and R. W. Murray, *J. Am. Chem. Soc.*, 2008, **130**, 3754–3755.
4 H. Qian, W. T. Eckenhoff, Y. Zhu, T. Pintauer and R. Jin, *J. Am. Chem. Soc.*, 2010, **132**, 8280–8281.
5 R. Jin, *Nanoscale*, 2010, **2**, 343–362.
6 K. M. Harkness, D. E. Cliffel and J. A. McLean, *Analyst*, 2010, **135**, 868–874.

7 J. B. Tracy, G. Kalyuzhny, M. C. Crowe, R. Balasubramanian, J. P. Choi and R. W. Murray, *J. Am. Chem. Soc.*, 2007, **129**, 6706–6707.
8 H. Qian and R. Jin, *Nano Lett.*, 2009, **9**, 4083–4087.
9 C. A. Fields-Zinna, R. Sardar, C. A. Beasley and R. W. Murray, *J. Am. Chem. Soc.*, 2009, **131**, 16266–16271.
10 O. Lopez-Acevedo, J. Akola, R. L. Whetten, H. Gronbeck and H. Hakkinen, *J. Phys. Chem. C*, 2009, **113**, 5035–5038.
11 T. G. Schaaff, M. N. Shafigullin, J. T. Khoury, I. Vezmar and R. L. Whetten, *J. Phys. Chem. B*, 2001, **105**, 8785–8796.
12 Y. Sun and Y. Xia, *Analyst*, 2003, **128**, 686–691.
13 H. Hiramatsu and F. E. Osterloh, *Chem. Mater.*, 2004, **16**, 2509–2511.
14 R. Ferrando, J. Jellinek and R. L. Johnston, *Chem. Rev.*, 2008, **108**, 845–910.
15 M. J. Hostetler, C. J. Zhong, B. K. H. Yen, J. Anderegg, S. M. Gross, N. D. Evans, M. Porter and R. W. Murray, *J. Am. Chem. Soc.*, 1998, **120**, 9396–9397.
16 S. Link, Z. L. Wang and M. A. El-Sayed, *J. Phys. Chem. B*, 1999, **103**, 3529–3533.
17 M. P. Mallin and C. J. Murphy, *Nano Lett.*, 2002, **2**, 1235–1237.
18 J. Wilcoxon, *J. Phys. Chem. B*, 2008, **113**, 2647–2656.
19 C. M. Gonzalez, Y. Liu and J. C. Scaiano, *J. Phys. Chem. C*, 2009, **113**, 11861–11867.
20 C. A. Fields-Zinna, M. C. Crowe, A. Dass, J. E. F. Weaver and R. W. Murray, *Langmuir*, 2009, **25**, 7704–7710.
21 Y. Negishi, W. Kurashige, Y. Niihori, T. Iwasa and K. Nobusada, *Phys. Chem. Chem. Phys.*, 2010, **12**, 6219–6225.
22 Y. Negishi, T. Iwai and M. Ide, *Chem. Commun.*, 2010, **46**, 4713–4715.
23 A. Dass, A. Stevenson, G. R. Dubay, J. B. Tracy and R. W. Murray, *J. Am. Chem. Soc.*, 2008, **130**, 5940–5946.
24 A. Dass, K. Holt, J. F. Parker, S. W. Feldberg and R. W. Murray, *J. Phys. Chem. C*, 2008, **112**, 20276–20283.
25 T. G. Schaaff, M. N. Shafigullin, J. T. Khoury, I. Vezmar, R. L. Whetten, W. G. Cullen, P. N. First, C. GutierrezWing, J. Ascensio and M. J. JoseYacaman, *J. Phys. Chem. B*, 1997, **101**, 7885–7891.
26 A. C. Dharmaratne, T. Krick and A. Dass, *J. Am. Chem. Soc.*, 2009, **131**, 13604–13605.
27 H. Qian, Y. Zhu and R. Jin, *ACS Nano*, 2009, **3**, 3795–3803.
28 R. J. Arnold and J. P. Reilly, *J. Am. Chem. Soc.*, 1998, **120**, 1528–1532.
29 R. B. Wyrwas, M. M. Alvarez, J. T. Khoury, R. C. Price, T. G. Schaaff and R. L. Whetten, *Eur. Phys. J. D*, 2007, **43**, 91–95.
30 M. M. Alvarez, J. T. Khoury, T. G. Schaaff, M. N. Shafigullin, I. Vezmar and R. L. Whetten, *J. Phys. Chem. B*, 1997, **101**, 3706–3712.
31 J. Farges, M. F. de Feraudy, B. Raoult and G. Torchet, *J. Chem. Phys.*, 1986, **84**, 3491–3501.
32 E. G. Mednikov, M. C. Jewell and L. F. Dahl, *J. Am. Chem. Soc.*, 2007, **129**, 11619–11630.
33 N. T. Tran, D. R. Powell and L. F. Dahl, *Angew. Chem., Int. Ed.*, 2000, **39**, 4121–4125.